COMMISSIONS 27 AND 42 OF THE IAU
INFORMATION BULLETIN ON VARIABLE STARS

Number 6134

Konkoly Observatory
Budapest
30 March 2015

HU ISSN 0374 – 0676

LO ANDROMEDAE – A W-TYPE OVERCONTACT ECLIPSING BINARY

NELSON, ROBERT H.[1,2]; ROBB, RUSSELL M.[2,3]

[1] 1393 Garvin Street, Prince George, BC, Canada, V2M 3Z1, email: bob.nelson@shaw.ca

[2] Guest investigator, Dominion Astrophysical Observatory, Herzberg Institute of Astrophysics, National Research Council of Canada

[3] Department of Physics and Astronomy, University of Victoria, Victoria, B.C., Canada, V8P 2W7

The variability of LO And (= TYC 3637-416-1= NSV 14569 = NSVS 3561083 = CSV 8853 = WR 136) was discovered photographically by Weber (1963), who classified the system as a probable Cepheid variable. Diethelm & Gautschy (1980) determined a period of 0.190429 days (half the modern value) and supplied a full photoelectric light curve displaying only one minimum. The General Catalogue of Variable Stars (Samus et al., 1985-2013) lists the type as EW and a period of 0.3804427 days, with a reference to Kreiner (2004). From 1995 to 2014 there have been numerous eclipse timings. Gürol & Müyesseroğlu (2005) [hereafter G&M (2005)] presented five new times of minima of their own, collected a total of 15 photographic (pg), 164 visual (vis), 17 photoelectric (PE), and 10 charge-coupled device (CCD) eclipse timings from the literature, and performed the first period study of the system. Plotting an eclipse timing (ET) diagram (a.k.a. O−C diagram), they first determined a quadratic fit (which they attributed to mass exchange), noting that it was not sufficient to explain the period variation completely. They then went on to solve for the parameters of the orbit of the putative third star, listed in Table 1. (They considered, then rejected, that an alternate explanation might be magnetic cycles – the Applegate effect (Applegate, 1992)).

Assuming that the residual variation is due to the light time effect (LTE) resulting from a third orbiting body, the new times of minima, T can be predicted by the equation

$$T = \mathrm{HJD}_0 + P_0 E_0 + (c_0 + c_1 E + c_2 E^2) + \Delta T \qquad (1)$$

where HJD_0 (= 24 45071.059) is the starting epoch, P_0 (= 0.38043556 days) is initial period, c_0, c_1 and c_2 are the coefficients for the quadratic fit, and ΔT is the time delay due to orbital motion of the close eclipsing pair about the centre of mass of the triple system. The latter is given by (Irwin, 1952, 1959):

$$\Delta = A \frac{(1 - e^2)\sin(\nu + \omega)}{(1 + e\cos\nu) + e\sin\omega} \qquad (2)$$

where A = semi-amplitude = $\frac{1}{2}[(\mathrm{O-C})_{\max} - (O-C)_{\min}] = (a_{13}\sin i_3)/c$; i_3 = inclination of the 3rd star orbit (90°= edge-on); e = eccentricity; ν = true anomaly; c = speed of light, and ω = argument of periastron.

Quantity	G&M (2004)	This study	unit
Constant, c_0	1.00	4.68	10^{-3} days
Slope, c_1	0	−9.69	10^{-6} days/cycle
Quadratic coeff., c_2	1.281	1.167	10^{-10} days/cycle^2
Amplitude, $A = a_{13} \sin i/c$	0.00829	0.00755	days
$a_{13} \sin i$	1.435	1.31	astron. units
Eccentricity, e	0.275	0.262	—
Period, P_3	37.08	29.6	years
Arg. of periastron, ω	198	80.4	degrees
Periastron time, $T_{\rm p}$	41919.1	46431.0	HJD−2400000
dP/dt	2.46	2.24	10^{-7} days/year
Mass transfer rate, dm_1/dt	+1.686	+1.537	10^{-7} $M_\odot$/year
Mass function, $f(m_3)$	0.002150	0.00256	$M_\odot$
Mass, m_3	0.21	0.22	$M_\odot$

Table 1: Parameters for the quadratic + LTE fit from the analysis of G&M (2005) and the present paper, plus some derived quantities.

With the benefit of 48 new PE and CCD subsequent eclipse timings, we have re-determined a quadratic + LTE fit using the linear elements (HJD$_0$, P_0) given above; both sets of resulting parameters are given in Table 1, column 3. An ET difference plot is displayed in Figure 1. Weights of 0.1 were assigned to the visual estimates, and 1 to the photographic, photoelectric and CCD eclipse timings. The residuals from quadratic fits of both studies are displayed in Figs. 2 and 3. (Note that the latter two cannot be displayed in the same figure because constants c_0, c_1 and c_2 are different in each case.)

It will be seen that, visually, the present solution fits the augmented data set better than that of G&M (2005). As in their work, we have solved for the intrinsic rate of period change, dP/dt by equation 3.

$$\frac{dP}{dt} = 2c_2 \left(\frac{365.24}{P_0}\right) \ . \tag{3}$$

One can show, under the conditions of mass and angular momentum conservation for the system as a whole, for masses m_1, m_2 and period P, that:

$$(m_1 m_2)^3 P = \text{constant} \tag{4}$$

Therefore, differentiating equation 4, one obtains:

$$\frac{dm_1}{dt} = \frac{1}{3P\left(\frac{1}{m_2} - \frac{1}{m_1}\right)} \frac{dP}{dt} \ . \tag{5}$$

Both values of dm_1/dt (from G&M (2005) and from this work) are presented in Table 1.

We have also solved for the mass function defined in Mayer (1990), assuming that the orbital inclination of the third-star orbit, i_3 is the same as the inclination of the binary pair orbit, i given in Table 5.

$$f(m_3) = \frac{(a_{13} \sin i)^3}{P_3^2} = \frac{(m_3 \sin i_3)^3}{(m_1 + m_2 + m_3)^2} \ . \tag{6}$$

From equation (6) one can iterate for m_3:

$$m_3 = \frac{a_{13} \sin i_3}{\sin i_3} \left(\frac{m_1 + m_2 + m_3}{P_3} \right)^{\frac{2}{3}} \quad . \tag{7}$$

The corresponding values for m_3 are also presented in Table 1.

It should be firmly borne in mind, however, that – due to the scatter in the early timings (before cycle 10000) – all the fit parameters and derived quantities are very tentative, and that new data over the next decade or so may very well render their values obsolete. By comparison, a much more robust quadratic + LTE fit, in the case of ER Orionis, may be found in Nelson (2015). The O−C file for LO And may be obtained from the AAVSO website (Nelson, 2013).

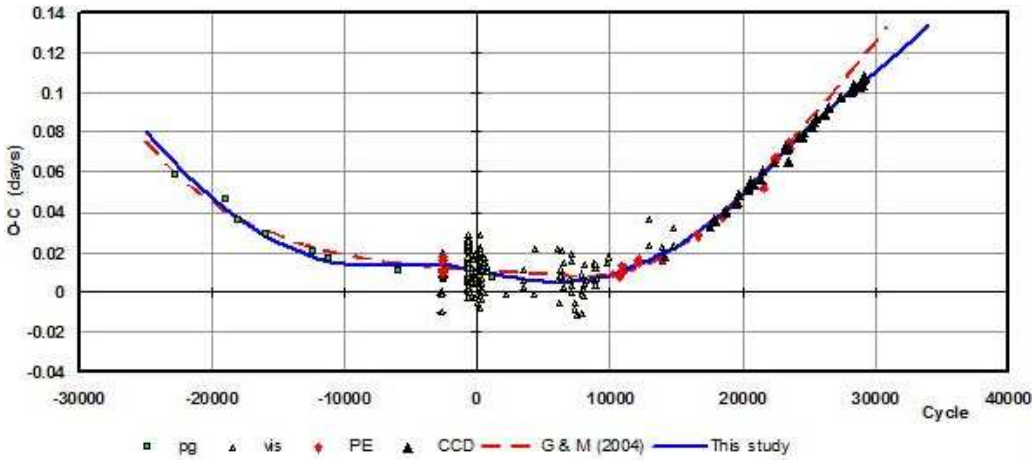

Figure 1. Eclipse timing diagram for LO And showing the fit of G&M (2005) [dashed line] and that of the present study [solid line].

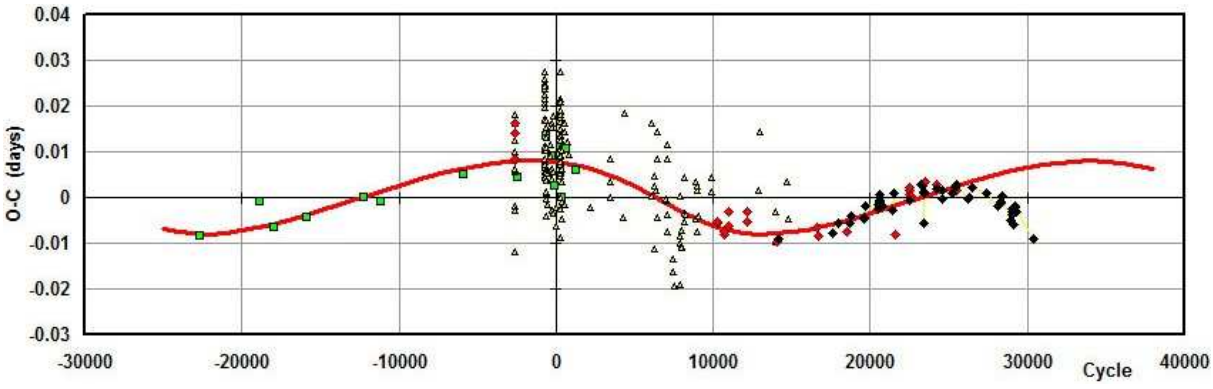

Figure 2. Residuals from the quadratic fit of G&M (2005) plus their LTE fit. See Fig. 1 for the legend.

Using the 2003 Wilson-Devinney code (see references below), G&M (2005) went on to perform a light curve analysis on B & V photometric data that they had obtained at Ankara University Observatory. They determined a value for the important parameter mass ratio ($q = m_2/m_1$) indirectly by the "q-search" method. [The latter entails fixing

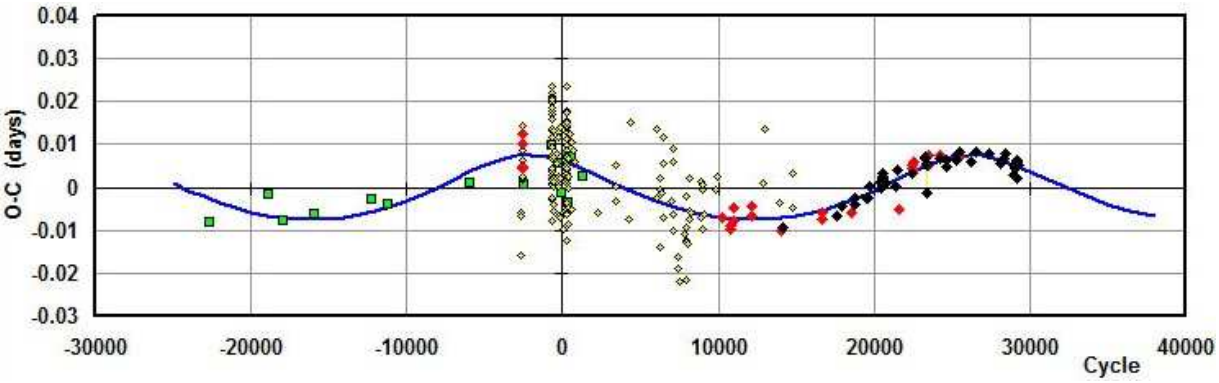

Figure 3. Residuals from the quadratic fit of this study plus our LTE fit. See Fig. 1 for the legend.

the mass ratio for a range of values, varying the remaining parameters (such as orbital inclination i, temperature T_2, system potential Ω, light value L_1, and – if used – spot parameters) to obtain solutions. The residuals from the best fit obtained in each case versus the corresponding value of q are plotted, and the q corresponding to the minimum is adopted.] The problem with the q-search method is that the value of q obtained is not as robust as that obtained spectroscopically, and, in the case of overcontact binaries undergoing partial eclipses, the value of q obtained is only determinable to about $\pm$10%. (Terrell & Wilson, 2005).

In order to improve on this study, one of the authors (R.H.N.) secured, in the months of September in 2007, 2009, 2010, and 2013, a total of 13 medium resolution ($R \sim 10000$ on average) spectra of LO And at the Dominion Astrophysical Observatory (DAO) in Victoria, British Columbia, Canada using the Cassegrain spectrograph attached to the 1.85 m Plaskett Telescope. He used the 21181 grating with 1800 lines/mm, blazed at 5000 Å giving a reciprocal linear dispersion of 10 Å/mm in the first order. The wavelength ranged from 5000 to 5260 Å, approximately. A log of observations is given in Table 2. The following elements were used for both RV and photometric phasing:

$$\text{JD (Hel) Min I} = 24\ 56226.6792 + 0.380441888458\ E \tag{8}$$

Frame reduction was performed by software RaVeRe (Nelson 2009). See Nelson et al. (2014) for further details. Radial velocities were determined using the Rucinski broadening functions (Rucinski, 2004, Nelson, 2010b, Nelson et al., 2014). An Excel worksheet with built-in macros (written by him) was used to do the necessary radial velocity conversions to geocentric and back to heliocentric values (Nelson 2010a). The resulting RV determinations are also presented in Table 2. These results were corrected 7.7% up in this case to allow for the small phase smearing. Correction was achieved by dividing the RVs by the factor $f = (\sin X)/X$; where $X = 2\pi t/P$ and t denotes exposure time, and P denotes the orbital period. For spherical stars, this correction is exact; in other cases, it can be shown to be close enough for any deviation to fall below observational errors. The mean rms error for each RV is 8.3 km/s and the rms deviation from the curves of best fit is 11.4 km/s. The best fit yielded the values $K_1 = 76.4(2.8)$ km/s, $K_2 = 272.4(3.3)$ km/ s and $V_\gamma = 3.7(1.9)$ km/s.

In May-July of 2012, the same author (R.H.N.) took a total of 169 frames in V, 172 in R_c (Cousins) and 169 in the I_c (Cousins) band at his private observatory in Prince George, BC, Canada. The telescope was a 33 cm f/4.5 Newtonian on a Paramount ME

DAO Image #	Mid Time (HJD−2400000)	Exposure (sec)	Phase at Mid-exp	V_1 (km/s)	V_2 (km/s)
11183	54365.9451	3600	0.019	1.7	—
11188	54365.9897	3600	0.136	−58.9	185.1
11203	54366.9663	3600	0.703	62.8	−256.0
11205	54367.0166	3600	0.835	76.2	−248.9
11211	54367.6466	3600	0.491	−2.6	—
11213	54367.6717	617	0.557	19.7	—
11219	54367.7539	3600	0.773	69.5	−259.5
11262	54369.8917	3600	0.393	−45.5	—
19073	55100.8404	3600	0.708	86.7	−277.8
19149	55102.9667	3600	0.297	−68.6	247.2
17272	55469.6910	3600	0.240	−69.8	278.2
9670	56545.9697	3600	0.262	−91.1	258.3
9692	56546.9266	3600	0.778	67.7	−294.9

Table 2: Log of DAO observations

Object	GSC	RA (J2000)	Dec (J2000)	V (mag)	$B-V$ (mag)
Variable	3637-0416	$23^{\rm h}27^{\rm m}06\overset{\rm s}{.}672$	$45°33'22\overset{''}{.}00$	11.25	+0.70
Comparison	3637-0299	$23^{\rm h}26^{\rm m}26\overset{\rm s}{.}518$	$45°30'37\overset{''}{.}77$	10.53	+1.00
Check	3636-0116	$23^{\rm h}25^{\rm m}56\overset{\rm s}{.}429$	$45°32'28\overset{''}{.}82$	10.18	+1.26

Table 3: Details of variable, comparison and check stars.

mount; the camera was an SBIG ST-10XME. Standard reductions were then applied. The comparison star (the same as for G&M, 2005) and check star are listed in Table 3. The coordinates and magnitudes are from the Tycho Catalogue, Hog et al. (2000).

For classification purposes, one of the authors (R.M.R.) took two low resolution spectra, on 2013 March 9 (HJD=24 56360.4608) and 2013 June 22 (HJD=24 56465.3077). He used the 1.85 m Plaskett telescope at the Dominion Astrophysical Observatory (DAO) in Victoria, British Columbia, Canada with the Cassegrain spectrograph in the 2131 configuration, resulting in a reciprocal dispersion of 60 Å/mm. The two spectra were very similar. The strength of the Calcium H&K lines, G-band, Hγ, Fe I 4384, Ca I 4227, and Hδ lines all indicated a F5 $\pm$1 spectral classification for LO And.

R.H.N. used the 2003 version of the Wilson-Devinney (WD) light curve and radial velocity analysis program with Kurucz atmospheres (Wilson and Devinney, 1971, Wilson, 1990, Kallrath, et al., 1998) as implemented in the Windows front-end software WDwint (Nelson, 2009) to analyse the data. To get started, the spectral type F5 V, mentioned above, was adopted. Interpolated tables from Cox (2000) gave a temperature $T1 = 6650 \pm 100$ K and $\log g = 4.355$. An interpolation program by Terrell (1994, available from Nelson 2009) gave the Van Hamme (1993) limb darkening values; and finally, a logarithmic (LD=2) law for the limb darkening coefficients was selected, appropriate for temperatures < 8500 K (ibid.).

From the GCVS 4 designation (EW) and from the shape of the light curve, mode 3 (overcontact binary) mode was used. Early on, it was noted that the maxima between eclipses were unequal. This is the O'Connell effect (Davidge & Milone, 1984, and

Band	x_1	x_2	y_1	y_2
Bol	0.640	0.641	0.243	0.243
V	0.705	0.705	0.280	0.280
R_c	0.632	0.632	0.287	0.287
I_c	0.549	0.548	0.275	0.275

Table 4: Limb darkening values from Van Hamme (1993)

WD Quantity	G & M Value	G & M error	This work Value	This work error	Unit
Temperature, T_1	6500	[fixed]	6650	[fixed]	K
Temperature, T_2	6465	184	6690	24	K
$q = m_2/m_1$	0.371	0.002	0.305	0.004	—
Potential, $\Omega_1 = \Omega_2$	2.548	0.026	2.401	0.009	—
Inclination, i	78.67	0.62	80.1	0.6	deg
Semi-maj. axis, a	—	—	2.74	0.02	sol. rad.
V_γ	—	—	-3.0	0.8	km/s
Spot co-latitude	—	—	97	10	deg
Spot longitude	—	—	45	5	deg
Spot radius	—	—	33	2	deg
Spot temp factor	—	—	0.9765	0.005	—
$L_1/(L_1 + L_2)(V)$	0.7061	0.0025	0.7330	0.0010	—
$L_1/(L_1 + L_2)(R_c)$	na	na	0.7339	0.0009	—
$L_1/(L_1 + L_2)(I_c)$	na	na	0.7348	0.0008	—
r_1 (pole)	0.4524	0.0058	0.4706	0.0003	orb. rad.
r_1 (side)	0.4873	0.0081	0.5103	0.0005	orb. rad.
r_1 (back)	0.5189	0.0115	0.5414	0.0008	orb. rad.
r_2 (pole)	0.2911	0.0099	0.2795	0.0012	orb. rad.
r_2 (side)	0.3055	0.0124	0.2937	0.0015	orb. rad.
r_2 (back)	0.3501	0.0251	0.3427	0.0035	orb. rad.
Phase shift	—	—	-0.0012	0.0004	—
$\Sigma\omega^2_{res}$	0.04039	—	0.02872	—	—

Table 5: Wilson-Devinney parameters

references therein) and is usually explained by the presence of one or more star spots. Accordingly, one was added first to star 1, and this gave good results. (Moving the spot to star 2 gave poorer results and was abandoned.)

Convergence by the method of multiple subsets was reached in a small number of iterations. (The subsets were: (a, L_1), (T_2, q), and (V_γ, i, q). The spots were handled separately.) Convective envelopes for both stars were used, appropriate for cooler stars (hence values gravity exponent $g = 0.32$ and albedo $A = 0.500$ were used for each). Detailed reflections were tried, with $n_{ref} = 3$, but there was little – if any – difference in the fit from the simple treatment. The limb darkening coefficients are listed in Table 4. There are certain uncertainties in the process (see Csizmadia et al., 2013, Kurucz, 2002). On the other hand, the solution is weakly dependent on the exact values used.

The model is presented in Table 5. Note that estimating the uncertainties in temper-

Quantity	G & M Value	G & M Error	This work Value	This work Error	unit
Temperature, T_1	6500	[fixed]	6650	200	K
Temperature, T_2	6465	184	6690	200	K
Mass, m_1	1.31	0.18	1.468	0.048	$M_\odot$
Mass, m_2	0.49	0.07	0.447	0.022	$M_\odot$
Radius, R_1	1.30	0.05	1.40	0.01	$R_\odot$
Radius, R_2	0.85	0.14	0.84	0.01	$R_\odot$
$M_{\rm bol}$, 1	3.67	0.08	3.45	0.02	mag
$M_{\rm bol}$, 2	4.62	0.39	4.53	0.02	mag
$\log g_1$	4.32	0.71	4.32	0.01	cgs
$\log g_2$	4.26	0.75	4.24	0.01	cgs
Luminosity, L_1	2.70	0.08	3.44	0.06	$L_\odot$
Luminosity, L_2	1.13	0.35	1.27	0.02	$L_\odot$
Fill-out factor	0.306	—	0.398	0.062	—
Distance, r	—	—	343	45	pc

Table 6: Fundamental parameters

atures T_1 and T_2 are somewhat problematic. A common practice is to quote the temperature difference over half a spectral sub-class (assuming that the classification is good to one spectral sub-class, which precision might be rare). In addition, various different calibrations have been made (Cox, 2000, page 388-390 and references therein, and Flower, 1996), and the variations between the various calibrations can be significant. In our case the classification is ± one sub-class. Therefore, we propose to assign an uncertainty of ± 200 K to the absolute temperatures of each, which would roughly span this range. The modelling error in temperature T_2, relative to T_1, is indicated by the WD output to be much smaller, around 24 K.)

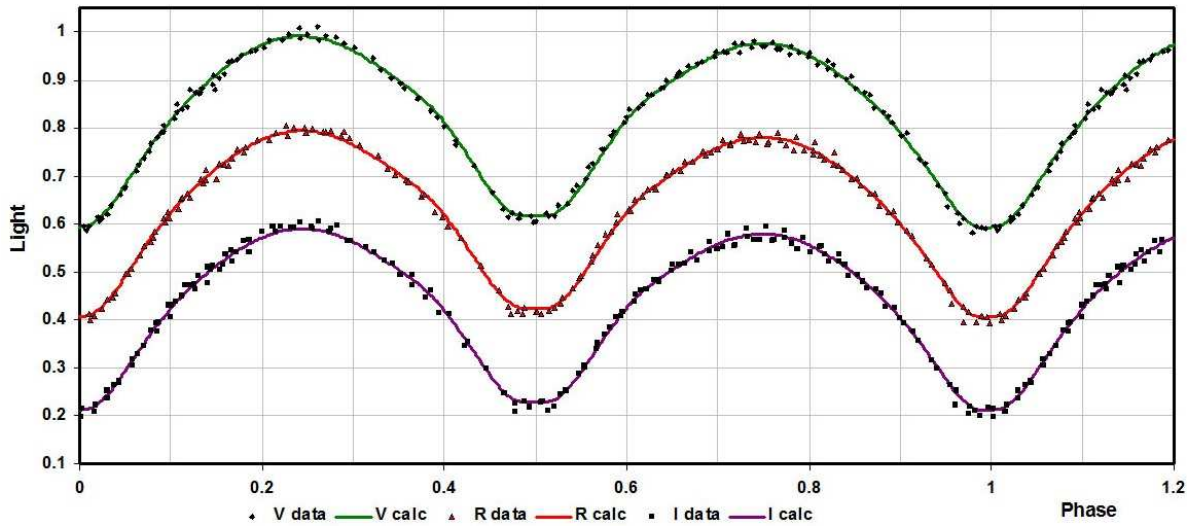

Figure 4. V, $R_{\rm c}$, and $I_{\rm c}$ light curves – data and WD fit

The WD output fundamental parameters and errors are listed in Table 6. Most of the errors are output or derived estimates from the WD routines. The fill-out factor $f = (\Omega^{\rm I} - \Omega)/(\Omega^{\rm I} - \Omega^{\rm O})$, where Ω is the modified Kopal potential of the system, $\Omega^{\rm I}$ is that of the inner Lagrangian surface, and $\Omega^{\rm O}$, that of the outer Lagrangian surface, was also calculated.

The light curve data and the fitted curves are depicted in Figure 4. The presence of third light was tested for, but found not to be significant.

The RVs are shown in Fig. 5. A three-dimensional representation from Binary Maker 3 (Bradstreet, 1993) is shown in Fig. 6.

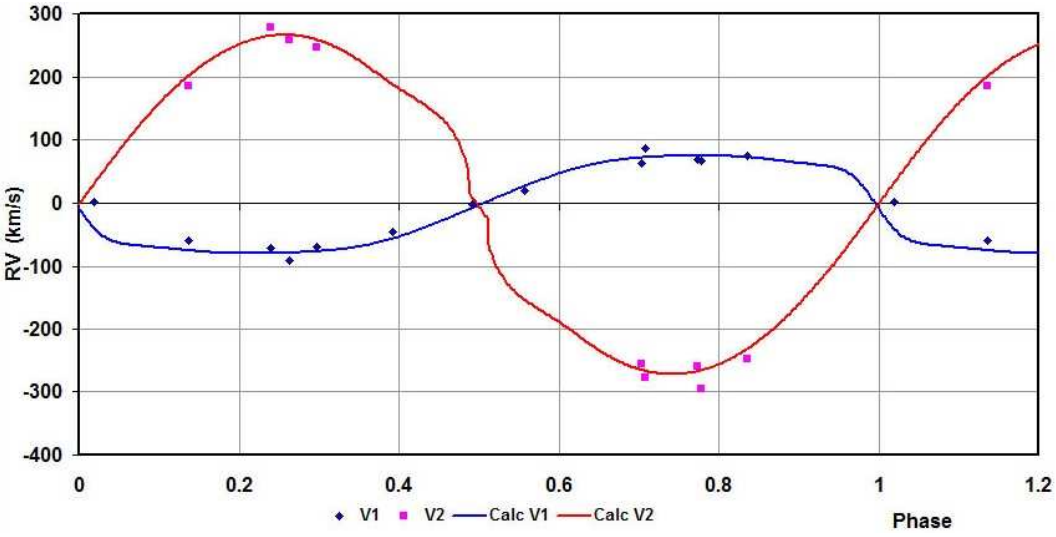

Figure 5. LO And: radial velocity curves – data and WD fit.

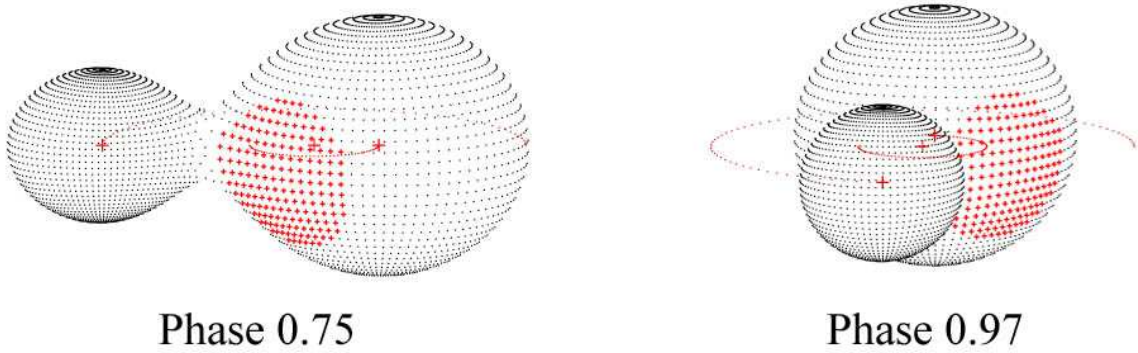

Figure 6. Binary Maker 3 representation of the system – at phases 0.75 and 0.97.

To determine the distance r in column 4, we proceeded as follows: First the WD routine gave the absolute bolometric magnitudes of each component; these were then converted to the absolute visual (V) magnitudes of both, $M_{V,1}$ and $M_{V,2}$, using the bolometric correction BC = −0.140 for each. The latter was taken from interpolated tables in Cox (2000). The absolute V magnitude was then computed in the usual way, getting M_V =

3.25 ± 0.03 magnitudes. The apparent magnitude in the V passband was $V = 11.19 \pm 0.09$, taken from the Tycho values (Hog et al., 2000) and converted to a Johnson magnitude using relations due to Henden (2001). The colour excess (in $B - V$) was obtained in the usual way, by subtracting the tabular value of $B - V$ (for that spectral class) from the observed (converted Tycho) value. This gave $E[B-V] = 0.26$ magnitudes. However, reference to the dust tables of Schlegel et al. (1998) revealed a value of $E[B-V] = 0.1711$ for those galactic coordinates. Since the $E[B-V]$ values have been derived from full-sky far-infrared measurements, they therefore apply to objects outside of the Galaxy; this value of $E[B-V]$ so derived then represents an upper limit for closer objects within the Galaxy. Hence the higher value of 0.26 cannot be regarded as reliable. Again, since the value of $E[B-V] = 0.1711$ represents an upper limit, objects closer than the edge of the galaxy should have a lower value; hence $E[B-V] = 0.086$ (half) was adopted and the error estimate also set to this value. Galactic extinction was obtained from the usual relation $A_V = RE[B-V]$, using $R = 3.1$ for the reddening coefficient. Hence, distance $r = 343$ pc was calculated from the standard relation:

$$r = 10^{0.2(V - M_V - A_V + 5)} \text{ parsecs} . \quad (9)$$

The errors were assigned as follows: $\delta M_{\rm bol,1} = \delta M_{\rm bol,2} = 0.02$, $\delta {\rm BC}_1 = \delta {\rm BC}_2 = 0.01$ (the variation of 1.5 spectral sub-classes), $\delta V = 0.09$, $\delta E(B-V) = 0.086$, all in magnitudes, and $\delta R = 0.1$. Combining the errors rigorously yielded an estimated error in r of 45 pc.

In conclusion, the fundamental parameters of this system have been determined. One of these is the mass ratio, defined by the WD routine as $q = m_2/m_1$. As to eclipse sub-type (A or W), the deeper eclipse, by convention, defines phase 0; therefore the star eclipsed at that phase – the primary – is the hotter one. However, in this case, detailed modelling using a spot results in a slightly higher temperature for the secondary, making the system type-W.

It is interesting to note that Gürol & Müyesseroğlu (2005), although they noted a magnitude difference in maxima (Max II − Max I) of -0.010 in V, made no attempt to include any spots in their WD modelling. They also the classified the system as type-A, which classification might have been different if they had added a spot as we have done. (However, in our case, we noted a magnitude difference (Max II − Max I) $\approx +0.03$ in the V band–the opposite. Clearly the spot, if it exists, has migrated in the time interval of nine years.)

Acknowledgements: It is a pleasure to thank the staff members at the DAO (especially Dmitry Monin and Les Saddlemyer) for their usual splendid help and assistance.

References:

Applegate, J.H., 1992, *ApJ*, **385**, 621

Bradstreet, D.H., 1993, "Binary Maker 2.0 - An Interactive Graphical Tool for Preliminary Light Curve Analysis", in Milone, E.F. (ed.) Light Curve Modelling of Eclipsing Binary Stars, pp 151-166 (Springer, New York, N.Y.)

Cox, A.N., ed, 2000, Allen's Astrophysical Quantities, 4th ed., (Springer, New York, NY)

Csizmadia, S., Pasternacki, T., Dreyer, C., Cabrera, A., Erikson, A. & Rauer, H., 2013, *A&A*, **549**, A9

Davidge, T.J., & Milone, E.F., 1984, *ApJS*, **55**, 571

Diethelm, R. & Gautschy, A., 1980, *IBVS*, **1767**

Flower, P.J., 1996, *ApJ*, **469**, 355
Gürol, B. & Müyesseroğlu, Z., 2005, *AN*, **326**, 43
Henden, A., 2001, http://www.tass-survey.org/tass/catalogs/tycho.old.html
Hog, E., et al., 2000, *A&A*, **355**, L27
Irwin, J.B., 1952, *ApJ*, **116**, 211
Irwin, J.B., 1959, *AJ*, **64**, 149
Kallrath, J., Milone, E.F., Terrell, D., and Young, A.T., 1998, *ApJ*, **508**, 308
Kreiner, J.M., 2004, *AcA*, **54**, 207
Kurucz, R.L., 2002, *BaltA*, **11**, 101
Mayer, P., 1990, *BAICz*, **41**, 231
Nelson, R.H., 2009, Software, by Bob Nelson,
http://members.shaw.ca/bob.nelson/software1.htm
Nelson, R.H., 2010a, Spreadsheets, by Bob Nelson,
http://members.shaw.ca/bob.nelson/spreadsheets1.htm
Nelson, R.H., 2010b, "Spectroscopy for Eclipsing Binary Analysis" in The Alt-Az Initiative, Telescope Mirror & Instrument Developments (Collins Foundation Press, Santa Margarita, CA), R.M. Genet, J.M. Johnson and V. Wallen (eds)
Nelson, R.H., 2013, Bob Nelsons O−C Files,
http://www.aavso.org/bob-nelsons-o-c-files
Nelson, R. H., Şenavcı, H.V. Baştürk, Ö. & Bahar, E., 2014, *NewA*, **29**, 57
Nelson, R.H., 2015, *NewA*, **34**, 159
Rucinski, S. M. 2004, "Advantages of the Broadening Function (BF) over the Cross-Correlation Function (CCF)", in Stellar Rotation, Proc. IAU Symp. 215., 14
Samus N.N., Durlevich O.V., Goranskij V.P., Kazarovets E. V., Kireeva N.N., Pastukhova E.N., Zharova A.V., 1985-2013, General Catalogue of Variable Stars
Schlegel, D.J., Finkbeiner, D.P. & Davis, M., 1998, *ApJ*, **500**, 525
Terrell, D., 1994, Van Hamme Limb Darkening Tables, vers. 1.1.
Terrell, D. & Wilson, R.E., 2005, *Ap&SS*, **296**, 221
Van Hamme, W., 1993, *AJ*, **106**, 2096
Weber, R., 1963, *IBVS*, **21**
Wilson, R.E., 1990, *ApJ*, **356**, 613
Wilson, R.E., & Devinney, E.J., 1971, *ApJ*, **166**, 605